BULLETIN OF THE POLISH ACADEMY OF SCIENCES
TECHNICAL SCIENCES, Vol. 69(6), 2021, Article number: e139317
DOI: 10.24425/bpasts.2021.139317

THERMODYNAMICS, MECHANICAL,
AERONAUTICAL ENGINEERING AND ROBOTICS

Numerical benchmarks for topology optimization of structures with stress constraints

Grzegorz FIUK and Mirosław W. MRZYGŁÓD*

Opole University of Technology, Faculty of Mechanical Engineering, ul. Mikołajczyka 5, 45-271 Opole, Poland

Abstract. Modern industry requires an increasing level of efficiency in a lightweight design. To achieve these objectives, easy-to-apply numerical tests can help in finding the best method of topological optimization for practical industrial applications. In this paper, several numerical benchmarks are proposed. The numerical benchmarks facilitate qualitative comparison with analytical examples and quantitative comparison with the presented numerical solutions. Moreover, an example of a comparison of two optimization algorithms was performed. That was a commonly used SIMP algorithm and a new version of the CCSA hybrid algorithm of topology optimization. The numerical benchmarks were done for stress constraints and a few material models used in additive manufacturing.

Key words: topology benchmarks; stress constraints; topology optimization; additive manufacturing.

1. INTRODUCTION

The automotive and aerospace industry requires an increasing level of efficiency in the design of novel structures. The fabrication by additive manufacturing (AM) plays an essential role in this technological race. Also, the design for additive manufacturing using topological optimization methodology is one of the fields of CAD/CAE engineering software that was subjected to rapid development in the last years. Thus, numerical benchmarks can help find the most robust, computationally efficient topology optimizing algorithms that are essential to support next-generation practical solutions of lightweight structures.

In Ochoa *et al.* [1], the authors perform a meta-analysis comparing 103 scientific articles according to the benchmark problems. Finally, they propose to unify stress topology optimization benchmarking, with rules of realistic dimensions, materials, and boundary conditions. Furthermore, Fanii *et al.* [2] compared different topology optimization algorithms with typical benchmark problems and concluded that the method of moving asymptotes should be used as the most flexible algorithm for structural topology optimization. Still, a range of asymptotes is needed to be increased in more extensive problems for computing timesaving. In the paper, Rojas-Labanda *et al.* [3] also compared different topology optimization algorithms, together with validating the performance of nonlinear optimization solvers for structural topology optimization. They conclude that the method of moving asymptotes (MMA), and the variant of globally convergent MMA are the most efficient and reliable. In the article, Yang *et al.* [4] proposed and compared two maximum stress constraint schemes for stress-based topology optimization. Presented stress correction – stability transformation method indicated application for minimization of the material in light-weighting designing. Researchers Pasini and colleagues [5] analyzed stress-constrained topology optimization for lattice structures. They proposed an optimization method used for lattice material treated as porous structures. It was shown that lattice cell topology and stress constraints had to impact the optimized distribution of density. In the paper, Lee *et al.* [6] presented stress-constrained optimization for self-weighted loads of structures. The authors compared mass and compliance-based optimization with stress constraints. Results showed that mass minimization optimization resulted in a globally more stressed structure. Also, to avoid converging into local minima, for self-weight problems with stress constraints, a special continuation method was proposed. In the article, Xia *et al.* [7] investigated and recommended the evolutionary topology optimization method for the stress minimization design of structures. They studied 2D and 3D structures with the filtering of sensitivity and topology variables to stabilize the optimization process. In the paper, Bulman *et al.* [8] compared homogenization methods, evolutionary methods, and hybrid methods of optimization for a series of benchmark problems, proposing their hybrid optimization algorithm. In the research, Rozvany [9, 10], as well as Rozvany and Lewiński [11], many analytical solutions for topology optimization benchmarks, were proposed. These solutions are commonly used as a verification of optimization algorithm. In the paper, Verbart *et al.* [12] proposed topology optimization with stress constraints, with the damage approach method. The results indicated that that new methodology could be used in structural problems. In the article, Goo *et al.* [13] analyzed the topology optimization of thin plates with stress constraints. Research provided a method for effectively controlling maximum stress by avoiding stress concentrations in notches. In the article, Holmberg *et al.* [14] and a Ph.D. dissertation [15], the author presents a method for stress-based optimization, also with fatigue constraints, for structural problems. They proposed a methodology for a shown methodology of designing optimal structures with fatigue and

*e-mail: m.mrzyglod@po.edu.pl

Manuscript submitted 2020-12-01, revised 2021-06-23, initially accepted for publication 2021-08-15, published in December 2021

stress constraints and uncertainties of loads. Also, the time-saving aspect of the computational cost of the optimization process was shown. In the article, Gilbert *et al.* [16] proposed a stress-constrained optimization method for the conceptual design of AM components.

In this paper, we present numerical benchmarks for topology optimization, and an example of a comparison of two optimization algorithms is presented. The benchmark proposed in the article is "two in one". They enable qualitative comparison with analytical examples (Michell structures) and quantitative comparison with the presented numerical solutions. The commonly used SIMP algorithm implemented in ANSYS and a new version of the Constant Criterion Surface Algorithm (CCSA) [17] is to be compared.

2. NUMERICAL BENCHMARKS FOR TOPOLOGY OPTIMIZATION

In this paper, two types of optimization algorithms were used for benchmarking, and they were as follows: density-based optimization, built on Solid Isotropic Material with Penalization (SIMP) [18,19], and hybrid algorithm – Constant Criterion Surface Algorithm (CCSA) [17,20].

The SIMP method discretizes the design domain, into a solid isotropic microstructure, with a penalization factor from 0 to 1, where 0 means removing material and 1 is for keeping material in design, based on density distribution. The discretized 0-1 optimization problem for the SIMP method with stress constraints could be described as follows [19]:

$$\begin{aligned} &\min_{\rho} \sum_{e=1}^{N} v_e \rho_e \\ \text{s.t.}\quad &\mathbf{K}\mathbf{u} = \mathbf{f}, \\ &(\sigma_e)_{VM} \le \overline{\sigma}, \\ &0 < \rho_{\min} \le \rho_e \le 1, \\ &e = 1,\ldots,N, \end{aligned} \tag{1}$$

where v_e are volumes, rho_e are the design variables (element densities), $\mathbf{K}$ is the stiffness matrix, $\mathbf{u}$ and $\mathbf{f}$ are the displacement and load vectors, $\rho_{\min}$ are lower bound on density, introduced to prevent singularity of the problem, $(\sigma_e)_{VM}$ is the von Mises equivalent stress, $\overline{\sigma}$ is the von Mises stress bound.

The CCSA is an evolutionary topology algorithm combined with a simulated annealing procedure, which can generate many quasi-optimal solutions during the optimization process. The CCSA discretized 0–1 optimization problem with constraints can be formulated as follows [17]:

$$\begin{aligned} &\min_{\eta} f(\eta_i) \\ \text{s.t.}\quad & g_j(x_i) \le \overline{g}_j, \quad j = [1, 2, \ldots, M], \end{aligned} \tag{2}$$

where: $x_i = [x_1, x_2, \ldots, x_N]$ is a set of finite elements,

$\eta_i = [\eta_1, \eta_2, \ldots, \eta_N]$ is a vector of design variables (pseudo-density of finite elements) defined as $\eta_i = E_{\min}$ or E_0, $E_{\min}$ and E_0 are minimum and real Young's modulus of the material of the structure, respectively, $g_j(x)$ are criterion parameters (e.g. equivalent stress, compliance, etc.) $\overline{g_j}$ are the bound of constraints.

The algorithm generates a solution through the iterative elimination of elements with a low value of the constraint criterion function (e.g. stress) (see Fig. 1a). This process is controlled

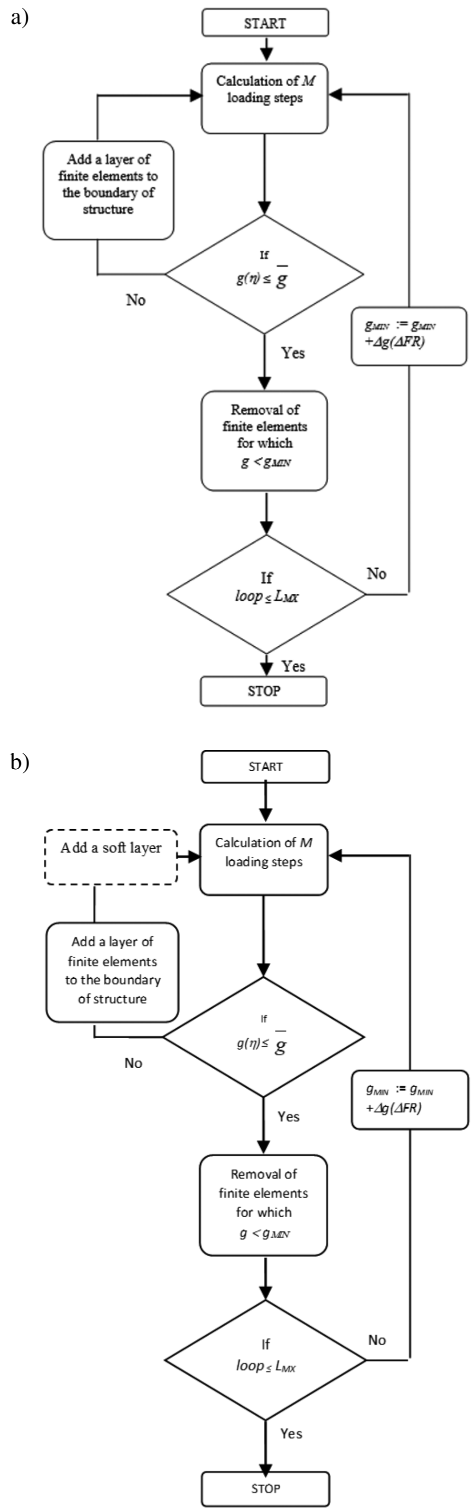

Fig. 1. The old version (a) and the new version of the CCSA algorithm (b)

by the constant percentage parameter of subtracted volumes ΔF and gives a possibility to set the optimization speed and additionally stabilizes the optimization process near the quasi-optimum. To achieve the constant value ΔF during each iteration, the boundary value of the constraint criterion $g_{\min}(\Delta F)$ is dynamically determined. When the criterion function is above the limit $\overline{g}$, a layer of finite elements is added to the entire boundary of the structure. The procedure of increasing the volume of the structure is continued until the criterion parameter g returns to admissible values. By increasing and decreasing the structure volume, the algorithm delivers better solutions after reaching the subsequent quasi-optimal solution.

In the present work, the new version of CCSA will be used. The CCSA algorithm was enriched with a new procedure of surrounding solutions through the layer of finite elements with the minimum value of the Young modulus $E_{\min}$ has been added (see Fig. 1b). The "soft layer" increases the stiffness of slender elements and improves the stability of the algorithm [20].

The CCSA algorithm was applied mostly to design optimization problems with stress or fatigue constraints. However, it was also used in finding solutions dedicated to additive manufacturing design, crashworthiness design, and optimization of transient thermomechanical loaded structures [17, 20–23].

All presented models were meshed using 20-nodes higher-order elements (SOLID185). The CCSA algorithm was limited to 1000 loops. All calculations were done at the workstation containing dual-CPU Intel Xeon E-5 2643 v2 with 96 GB of RAM.

3. THE L-SHAPED DOMAINS BENCHMARK

For the first benchmark, the L-shaped domains problem by Lewiński-Rozvany [24] was selected (see Fig. 2a). The design space dimension and boundary condition of the benchmark were shown in Figs. 2b and 2c. The thickness of the design space for the tested structures was selected arbitrarily, partly based on tests, to avoid buckling problems and at the same time not to extend the calculation times too much. Boundary conditions are applied indirectly through geometry (line, surface) and are evenly distributed over the numerical model. FE mesh properties were shown in Table 1. The commercial topological optimization methods based on the SIMP algorithm require a validation step in which a numerical solution containing intermediate density elements must be converted to a solid body with constant density. So, the use of 3D benchmark models for research seems to be justified. For this benchmark, a material model of steel was used, with Young modulus $E = 200$ GPa and Poisson ratio 0.3. The optimization process was conducted with the objective function in the form of volume minimization and with the equivalent stress constraints of 150 MPa.

The ANSYS/SIMP optimization workflow was presented (see Figs. 3a–3c). After performing the static analysis (Fig. 3a), the topology optimization was done (Fig. 3b). When the topology optimization procedure was finished, the quasi-optimum solution of design density was exported as an STL file to geometry rebuild in Space Claim-Geometry (Fig. 3c). Finally, the structural solution passes validation if it accomplishes assumed constraints. This step makes it difficult due to STL adapting process, where optimal design could be lost during facets cleaning and rebuilding to a solid model. Small notches can appear, affect final stress results, as shown in Fig. 4.

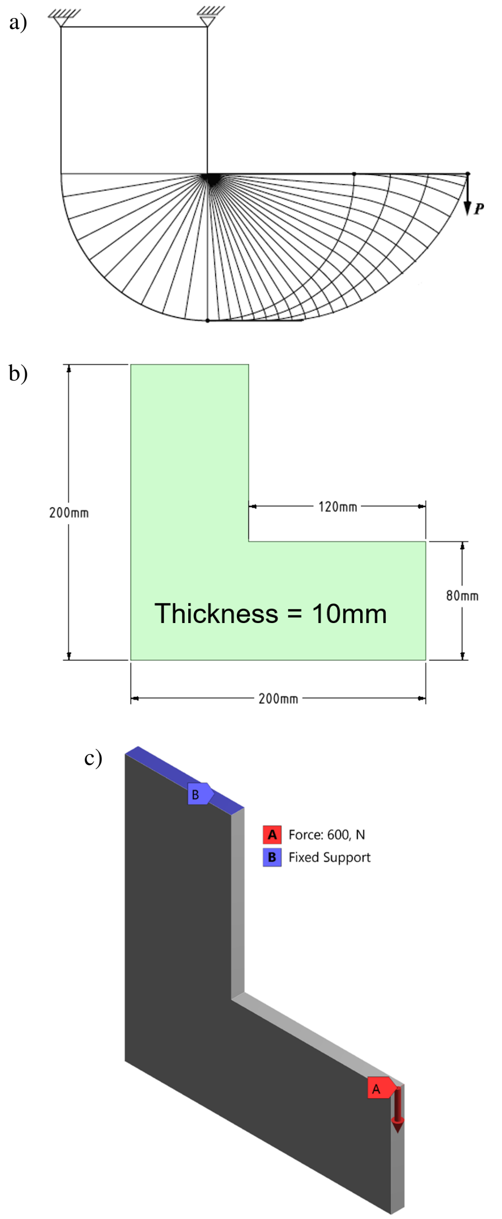

Fig. 2. The L-shaped domains benchmark: analytical solution of case of long-distance of the point P to the support (a) [23], the dimension of the design space (b), and boundary conditions for optimization (c)

Table 1
Mesh parameters

	Mesh parameters
Element size	1.5 mm
No. of elements	75 852
Type of element	Higher-order 3-D 20-node solid element (SOLID185)t

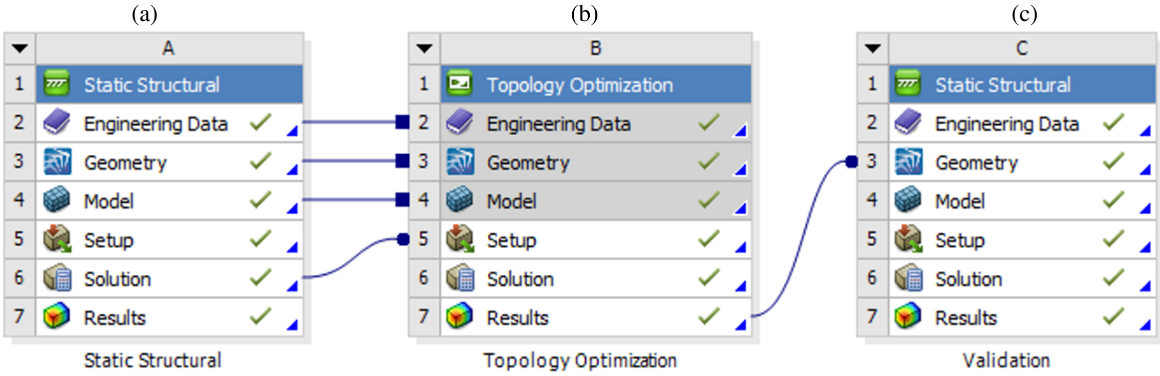

Fig. 3. Optimization workflow in ANSYS: "Static Structural" – preliminary FE analysis (a), "Topology Optimization" (b), "Static Structural" – validation of optimal solution (c)

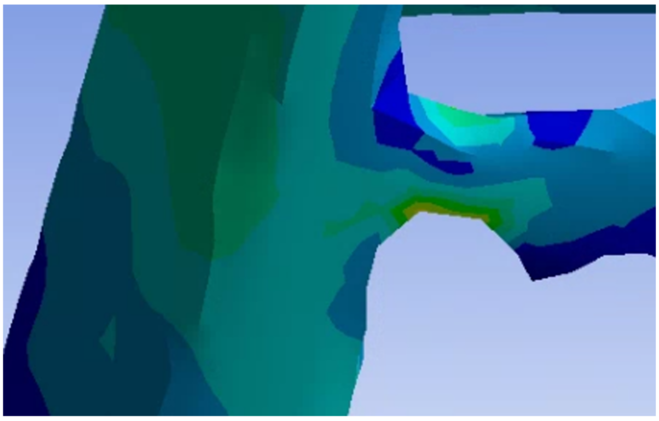

Fig. 4. Notch in model geometry after STL rebuild

For the CCSA algorithm, optimization results were shown in Fig. 5a. The optimum design is presented with a soft layer and the contour map of Huber–Mises–Hencky's equivalent stress (see Fig. 5b).

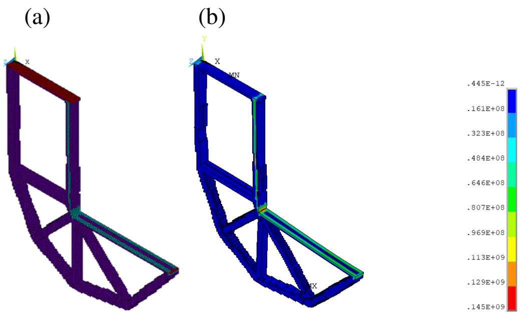

Fig. 5. The CCSA algorithm: the optimal structural solution with a soft layer (a), the contour map of Huber–Mises–Hencky's equivalent stress [Pa] (b)

All results were compared due to volume fraction % of the original volume of the design space, measured in mm^3. For the SIMP algorithm, the result was shown in Figs. 6 and 7. Figure 6 presents the solution that did not pass the validation step, with a maximum stress level of about 284 MPa and a volume fraction of about 7%. As presented, the optimized model had regions where the assumed constraints were not met (maximum equivalent stress of 150 MPa). For that reason, a few iterations of increasing the structure volume were performed to lower the stress level. The SIMP solution finally passed the validation step with the maximum equivalent stress of 103 MPa (see Fig. 7). In Table 2, a comparison of the objective function (the volume) and constraints (the maximum equivalent stress) between the CCSA and SIMP algorithm was shown. Furthermore, for the L-bracket benchmark, CCSA achieved better results with the lower value of volume and passed the validation step without corrections. Approximate times to find the solution was 3 h 41 minutes for CCSA, 3 h 28 minutes for the SIMP solution, and 10 h 58 minutes for SIMP to obtain a validated so-

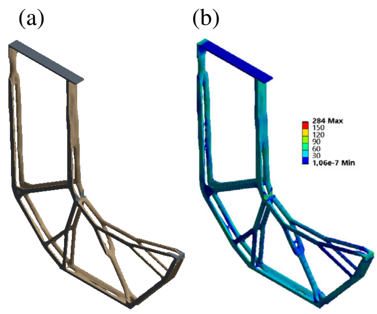

Fig. 6. The SIMP algorithm: the solution (a), the contour map of Huber–Mises–Hencky's equivalent stress [MPa] (b)

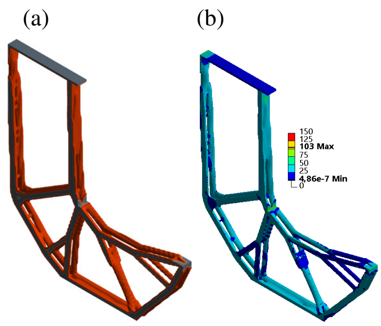

Fig. 7. The SIMP algorithm: the validated solution (a), the contour map of Huber–Mises–Hencky's equivalent stress [MPa] (b)

lution. The solutions for both methods differ. However, both solutions are similar to the analytical solution (see Fig. 2a), while the SIMP solution is more spatial.

Table 2
Results of optimization for the L-bracket problem

Algorithm	The objective function: volume fraction [%]	The constraints: maximum equivalent stress [MPa]
SIMP	7	284
SIMP after validation	11	103
CCSA	6	145

4. THE SQUARE-SHAPED LINE SUPPORT BEAM BENCHMARK

The square-shaped line support beam benchmark by Lewiński-Rozvany [11] was considered as the second optimization problem in this paper (see Fig. 8a). The dimension of the design space and applied boundary conditions were shown in Figs. 8b and 8c and mesh parameters in Table 3. The thickness for the design space was equal to 10 mm. For the investigation, the material model of PEI (Polyethylenimine) with Young modulus 2965 MPa and Poisson ratio 0.39 was assumed. The same optimization assumptions were made for both algorithms. The optimization process was conducted with the objective function in the form of volume minimization and with the equivalent stress constraints of 20 MPa.

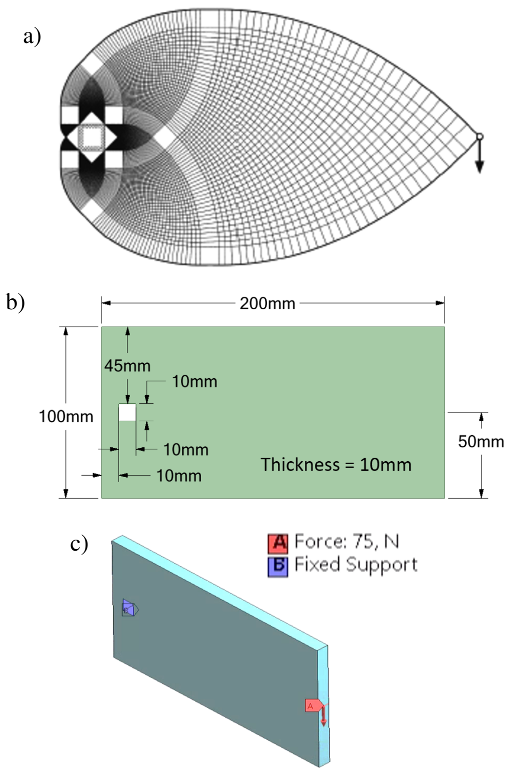

Fig. 8. The analytical solution of the Lewiński-Rozvany benchmark IV: analytical solution (a) [11], the dimension of the design space (b), and boundary conditions for optimization (c)

Table 3
Mesh parameters for the L–R beam

	Mesh parameters
Element size	2 mm
No. of elements	24 875
Type of element	Higher-order 3-D 20-node solid element (SOLID185)t

A comparison of optimization results was presented in Table 4. The solution of the SIMP algorithm of volume fraction about 8% and the maximum equivalent stress level of 53 MPa level was shown in Fig. 9. The validated solution, with an increased volume fraction of 16% and 14.5 MPa of maximum equivalent stress level, is presented in Fig. 10. The CCSA solution with a volume fraction of 6% and the maximum stress level of 19.2 MPa is presented in Fig. 11. Approximate times to find the solution were 1 h 50 minutes for CCSA, 1 h 03 minutes for the SIMP solution, and 2 h 30 minutes for SIMP validated solution.

Table 4
Results of optimization for the square-shaped line support beam problem

Algorithm	The objective function: volume fraction [%]	The constraints: maximum equivalent stress [MPa]
SIMP	8	52.6
SIMP after validation	16	14.5
CCSA	6	19.2

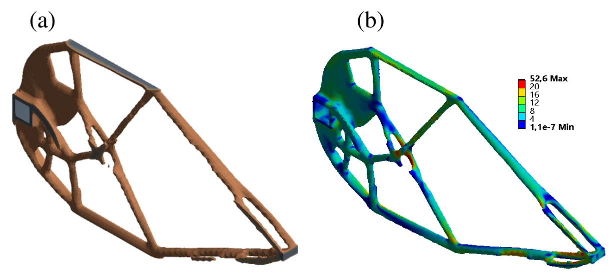

Fig. 9. The SIMP algorithm: the minimum volume of optimal structural solution (a), the contour map of Huber–Mises–Hencky's equivalent stress [MPa] (b)

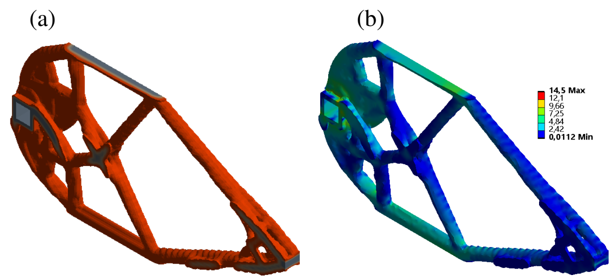

Fig. 10. The SIMP algorithm: the minimum volume of stress passed structural solution (a), the contour map of Huber–Mises–Hencky's equivalent stress [MPa] (b)

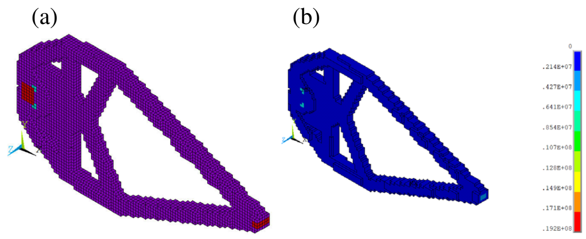

Fig. 11. The CCSA algorithm: the optimal structural solution with a soft layer (a), the contour map of Huber–Mises–Hencky's equivalent stress [Pa] (b)

5. THE "MBB BEAM" BENCHMARK PROBLEM

As a third benchmark, the *Messerschmitt–Bölkow–Blohm* beam problem [9, 25] was selected (see Fig. 12a). The dimension of the design space and applied boundary conditions were shown in Figs. 12b and 12c. The thickness of the design space was 10 mm. A material model of steel with Young modulus E = 200 GPa and Poisson ratio 0.3 was used. The mesh parameters were shown in Table 5. The optimization process was conducted with the objective function in the form of volume minimization and with the equivalent stress constraints of 100 MPa.

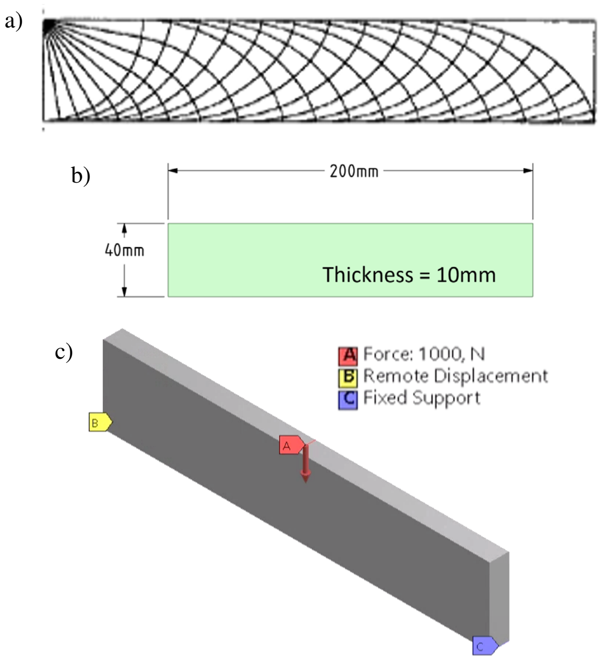

Fig. 12. The half analytical solution of the MBB beam benchmark: analytical solution (a) [25], the dimension of the design space (b), and boundary conditions for optimization (c)

Table 5
Mesh parameters for the L–R beam

	Mesh parameters
Element size	1 mm
No. elements	80 000
Type of element	Higher-order 3-D 20-node solid element (SOLID185)t

A comparison of the optimization result was presented in Table 6. The solution of the SIMP algorithm of volume fraction about 16% and the maximum equivalent stress level of 180 MPa level was shown in Fig. 13. The validated solution, with an increased volume fraction of 26% and 100 MPa of maximum equivalent stress level, is presented in Fig. 14. The CCSA solution with a volume fraction of 14% and the maximum stress level of 98.9 MPa is presented in Fig. 15. Approximate times to find the solution was 9 h 13 minutes for CCSA, 3 h 02 minutes for the SIMP solution, and 11 h 32 minutes for SIMP meeting the constraints.

Table 6
Results of the optimization of the MBB beam benchmark

Algorithm	The objective function: volume fraction [%]	The constraints: maximum equivalent stress [MPa]
SIMP	16	180
SIMP second validation	26	100
CCSA	14	98.9

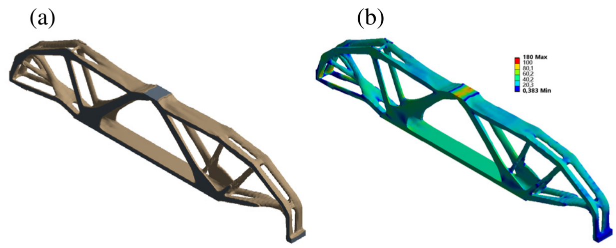

Fig. 13. The SIMP algorithm: the solution (a), the contour map of Huber–Mises–Hencky's equivalent stress [MPa] (b)

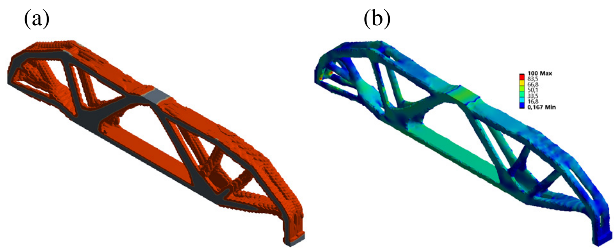

Fig. 14. The SIMP algorithm: the validated solution (a), the contour map of Huber–Mises–Hencky's equivalent stress [MPa] (b)

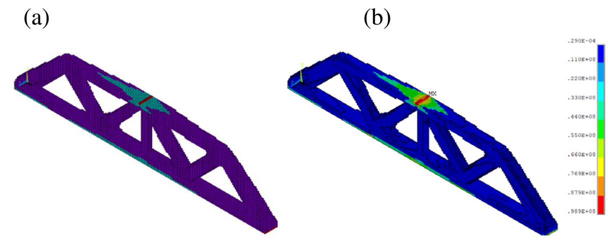

Fig. 15. The CCSA algorithm: the optimal structural solution with a soft layer (a), the contour map of Huber–Mises–Hencky's equivalent stress [Pa] (b)

6. MICHELL CANTILEVER BENCHMARK PROBLEM

As the last benchmark, the "Michell cantilever" problem [9, 26] was selected (see Fig. 16a). The dimension of the design space and applied boundary conditions were shown in Figs. 16b and 16c. The thickness of the design space was 10 mm. A material model of steel with Young modulus $E = 200$ GPa and Poisson ratio 0.3 was used. The mesh parameters were shown in Table 7. The optimization process was conducted with the objective function in the form of volume minimization and with the equivalent stress constraints of 50 MPa.

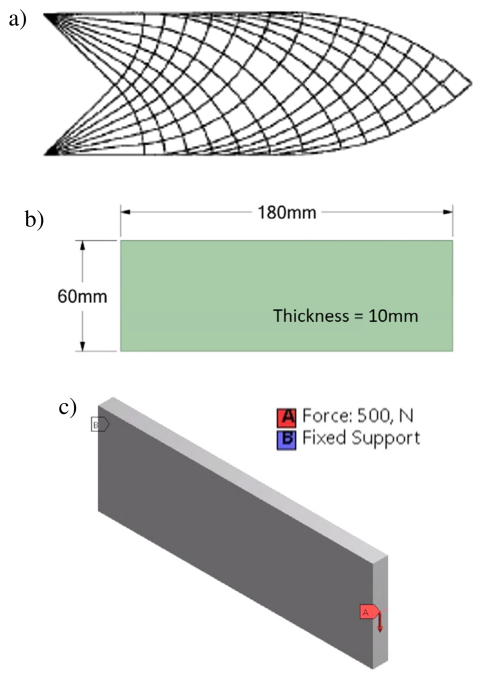

Fig. 16. The Michell cantilever benchmark: analytical solution (a) [25], the dimension of the design space (b), and boundary conditions for optimization (c)

Table 7

Mesh parameters for Michell cantilever benchmark

	Mesh parameters
Element size	1 mm
No. elements	108 000
Type of element	Higher-order 3-D 20-node solid element (SOLID185)t

A comparison of the optimization result was presented in Table 8. The solution of the SIMP algorithm of volume fraction about 19% and the maximum equivalent stress level of 75.2 MPa level was shown in Fig. 17. The validated solution, with an increased volume fraction of 25% and 45.5 MPa of maximum equivalent stress level, is presented in Fig. 18. The CCSA solution with a volume fraction of 21% and the maximum stress level of 48.8 MPa is presented in Fig. 19. Approximate times to find the solution was 7 h 16 minutes for CCSA, 3 h 37 minutes for the SIMP solution, and 7 h 37 minutes for SIMP validated solution.

Table 8

Results the optimization of Michell cantilever benchmark

Algorithm	The objective function: volume fraction [%]	The constraints: maximum equivalent stress [MPa]
SIMP	19	75.2
SIMP second validation	25	45.5
CCSA	21	48.8

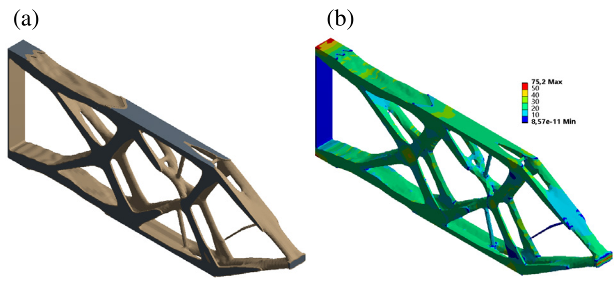

Fig. 17. The SIMP algorithm: the solution (a), the contour map of Huber–Mises–Hencky's equivalent stress [MPa] (b)

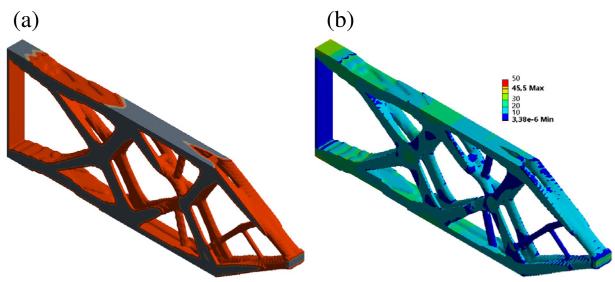

Fig. 18. The SIMP algorithm: the validated solution (a), the contour map of Huber–Mises–Hencky's equivalent stress [MPa] (b)

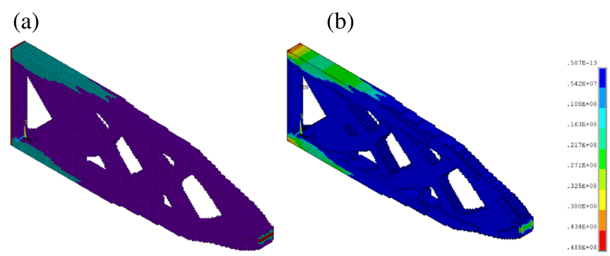

Fig. 19. The CCSA algorithm: the optimal structural solution with a soft layer (a), the contour map of Huber–Mises–Hencky's equivalent stress [Pa] (b)

7. DISCUSSION

The computation time of optimization of four numerical benchmarks is presented in Fig. 20. The authors assumed that it is important to present a comprehensive assessment of the results obtained. If the method requires validation (it is a clear recommendation of the software producer), we cannot omit this process and its "costs". Only in this way can we give a clear full picture of the application of the method. So, the computation time in-

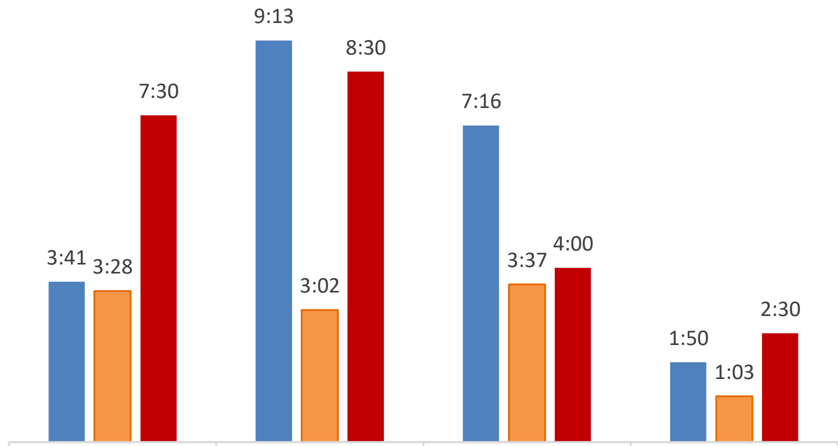

	L-shaped bracket	MBB beam	Michell cantilever	Lewiński-Rozvany beam
CSSA computation time	3:41	9:13	7:16	1:50
SIMP computation time	3:28	3:02	3:37	1:03
Time for SIMP validation steps	7:30	8:30	4:00	2:30

Fig. 20. Computation time of four numerical benchmarks [h]

cludes CCSA optimization time, SIMP optimization time, and the SIMP validation time. It should be noted the nearly "equal" computation times for SIMP solutions. This probably results from the algorithm characteristic in which the constraint conditions are met "smoothly" by adjusting element density. While the CCSA algorithm that gives "black and white" solutions, in case of exceeding the limits, must modify the structure (increase the volume evenly), which is a computationally expensive procedure. It can be pointed out that the SIMP algorithm had a lower computation time than CCSA, from a few minutes in the L-bracket case to 6 hours in the MBB problem.

However, summarized time for the SIMP method with validation and additional geometry adjustments presents higher values than CCSA, the algorithm makes validation "on-fly" during the optimization process, so the present time is summarized time for optimization and validation for finding the best solution in a range of loops. Most problems accrue during CAD rebuilding of SIMP optimization result, were satisfying keeping optimal result model, with reducing the amount of solid model faces for handling it by CAD software, where taking hours and needs a few runs to get an optimal result, that passes the validation step. This highly affects the process of design, especially for high-cost additive process manufacturing, where the unvalidated structure that goes to 3D printing could fail during quality check, even before any assembly tests.

It should also be mentioned that the CCSA algorithm produces many quasi-optimal alternative structural solutions that fulfil constraints. The algorithm is equipped with the procedure of restarting the search after reaching the subsequent quasi-optimal solution. This procedure uses a simulated annealing mechanism that is suitable for finding an optimal solution but also provides a set of alternative solutions [20]. In Fig. 21, 8 examples of alternative solutions were presented for the Lewiński-Rozvany beam benchmark. The presented solutions are equiva-

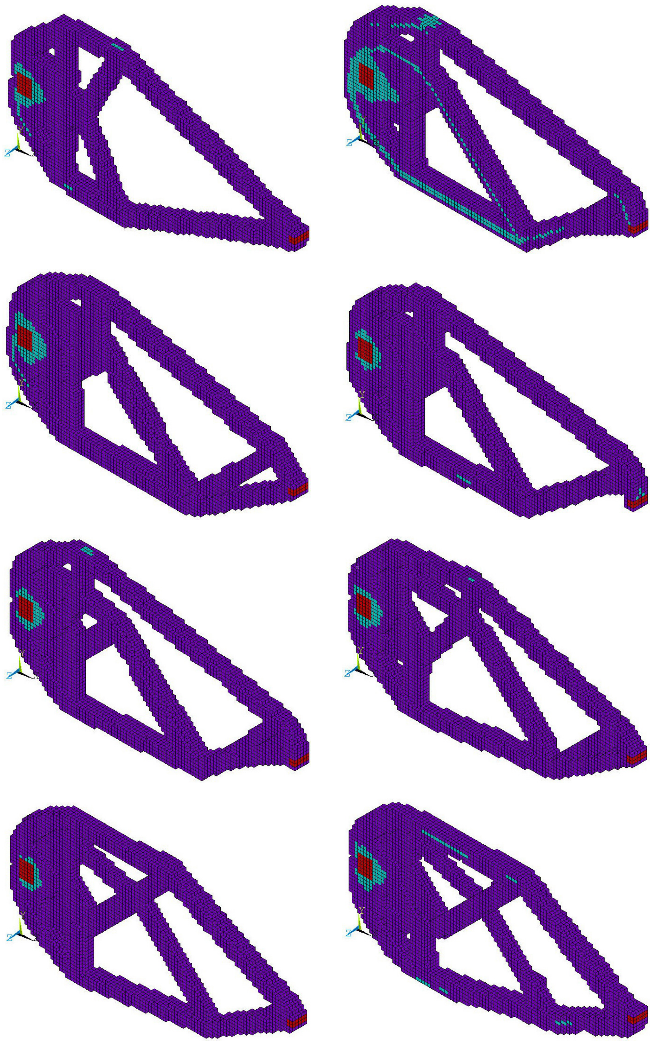

Fig. 21. Computation time of four numerical benchmarks [h]

lent. All of them meet the assumed limits and their mass varies within 1%. Obtaining such solutions is a unique property of the CCSA algorithm.

8. CONCLUSIONS

In this paper, four numerical benchmarks for the topology optimization of structures with stress constraints were proposed. The benchmarks are of type "two in one" and enabled qualitative and quantitative comparison.

The use of numerical benchmarks was illustrated by the example of a comparison of two optimizing algorithms using the three metal and one polyethyleneimine material models. That was a commonly used SIMP algorithm and the new version of the CCSA algorithm.

For both methods, results were like analytical solutions for Michell's trusses. For all four benchmarks, the primary solutions of SIMP needed to be improved in the time-consuming iterative procedure of geometry adjustments (validation) to fulfil stress constraints. The CCSA method makes validation "onfly", and can generate alternative quasi-optimal solutions.

Finding a methodology that could give an accurate proposal for designs dedicated to additive manufacturing could be crucial for the whole scale of the production industry, where minimizing energy consumption for the computation process, reduces the carbon footprint in all designing and manufacturing processes.

For future research, the biomimetic algorithm of topology optimization will be enriched with up-scaling methodology, which could increase the efficiency of searching for optimal structural solutions.

REFERENCES

[1] S.I. Valdez, S. Botello, M.A. Ochoa, J.L. Marroquín, and V. Cardoso, "Topology Optimization Benchmarks in 2D: Results for Minimum Compliance and Minimum Volume in Planar Stress Problems," *Arch. Comput. Methods Eng.*, vol. 24, no. 4, pp. 803–839, Nov. 2017, doi: 10.1007/s11831-016-9190-3.

[2] M. Fanni, M. Shabara, and M. Alkalla, "A Comparison between Different Topology Optimization Methods," *Bull. Fac. Eng. Mansoura Univ.*, vol. 38, no. 4, pp. 13–24, Jul. 2020, doi: 10.21608/bfemu.2020.103788.

[3] S. Rojas-Labanda and M. Stolpe, "Benchmarking optimization solvers for structural topology optimization," *Struct. Multidiscip. Optim.*, vol. 52, no. 3, pp. 527–547, Sep. 2015, doi: 10.1007/s00158-015-1250-z.

[4] D. Yang, H. Liu,W. Zhang, and S. Li, "Stress-constrained topology optimization based on maximum stress measures," *Comput. Struct.*, vol. 198, pp. 23–39, Mar. 2018, doi: 10.1016/j.comppstruc.2018.01.008.

[5] D. Pasini, A. Moussa, and A. Rahimizadeh, "Stress-Constrained Topology Optimization for Lattice Materials," in *Encyclopedia of Continuum Mechanics*, Berlin, Heidelberg: Springer Berlin Heidelberg, 2018, pp. 1–19.

[6] E. Lee, K.A. James, and J.R.R.A. Martins, "Stress-constrained topology optimization with design-dependent loading," *Struct. Multidiscip. Optim.*, vol. 46, no. 5, pp. 647–661, Nov. 2012, doi: 10.1007/s00158-012-0780-x.

[7] L. Xia, L. Zhang, Q. Xia, and T. Shi, "Stress-based topology optimization using bi-directional evolutionary structural optimization method," *Comput. Methods Appl. Mech. Eng.*, vol. 333, pp. 356–370, May 2018, doi: 10.1016/j.cma.2018.01.035.

[8] S. Bulman, J. Sienz, and E. Hinton, "Comparisons between algorithms for structural topology optimization using a series of benchmark studies," *Comput. Struct.*, vol. 79, no. 12, pp. 1203–1218, May 2001, doi: 10.1016/S0045-7949(01)00012-8.

[9] G.I.N. Rozvany, "Exact analytical solutions for some popular benchmark problems in topology optimization," *Struct. Optim.*, vol. 15, no. 1, pp. 42–48, Feb. 1998, doi: 10.1007/BF01197436.

[10] G.I.N. Rozvany, "A critical review of established methods of structural topology optimization," *Struct. Multidiscip. Optim.*, vol. 37, no. 3, pp. 217–237, Jan. 2009, doi: 10.1007/s00158-007-0217-0.

[11] T. Lewiński and G.I.N. Rozvany, "Analytical benchmarks for topological optimization IV: Square-shaped line support," *Struct. Multidiscip. Optim.*, vol. 36, no. 2, pp. 143–158, Aug. 2008, doi: 10.1007/s00158-007-0205-4.

[12] A. Verbart, M. Langelaar, and F. van Keulen, "Damage approach: A new method for topology optimization with local stress constraints," *Struct. Multidiscip. Optim.*, vol. 53, no. 5, pp. 1081–1098, May 2016, doi: 10.1007/s00158-015-1318-9.

[13] S. Goo, S. Wang, J. Hyun, and J. Jung, "Topology optimization of thin plate structures with bending stress constraints," *Comput. Struct.*, vol. 175, pp. 134–143, Oct. 2016, doi: 10.1016/ j.compstruc.2016.07.006.

[14] E. Holmberg, B. Torstenfelt, and A. Klarbring, "Stress constrained topology optimization," *Struct. Multidiscip. Optim.*, vol. 48, no. 1, pp. 33–47, Jul. 2013, doi: 10.1007/s00158-012-0880-7.

[15] E. Holmberg, *Topology optimization considering stress, fatigue and load uncertainties*. Linköping University Electronic Press, 2015.

[16] L. He, M. Gilbert, T. Johnson, and T. Pritchard, "Conceptual design of AM components using layout and geometry optimization," *Comput. Math. with Appl.*, vol. 78, no. 7, pp. 2308–2324, Oct. 2019, doi: 10.1016/j.camwa.2018.07.012.

[17] M. Mrzygłód, "Multi-constrained topology optimization using constant criterion surface algorithm," *Bull. Pol. Acad. Sci. Tech. Sci.*, vol. 60, no. 2, pp. 229–236, Oct. 2012, doi: 10.2478/v10175-012-0030-9.

[18] M. Zhou and G.I.N. Rozvany, "The COC algorithm, Part II: Topological, geometrical and generalized shape optimization," *Comput. Methods Appl. Mech. Eng.*, vol. 89, no. 1–3, pp. 309–336, Aug. 1991, doi: 10.1016/0045-7825(91)90046-9.

[19] M.P. Bendsøe and O. Sigmund, *Topology Optimization*. Berlin, Heidelberg: Springer Berlin Heidelberg, 2004.

[20] M.W. Mrzygłód, "Alternative quasi-optimal solutions in evolutionary topology optimization," in *AIP Conference Proceedings*, 2018, vol. 1922, p. 020007-1–020007-7, doi: 10.1063/1.5019034.

[21] G. Fiuk and M.W. Mrzygłód, "Topology optimization of structures with stress and additive manufacturing constraints," *J. Theor. Appl. Mech.*, vol. 58, no. 2, pp. 459–468, Apr. 2020, doi: 10.15632/jtam-pl/118899.

[22] M. Mrzygłód and T. Kuczek, "Uniform crashworthiness optimization of car body for high-speed trains," *Struct. Multidiscip. Optim.*, vol. 49, no. 2, pp. 327–336, Feb. 2014, doi: 10.1007/s00158-013-0972-z.

[23] P. Duda and M.W. Mrzygłód, “Shape and operation optimization of a thick-walled power boiler component,” in *MATEC Web of Conferences*, Nov. 2018, vol. 240, p. 05006, doi: 10.1051/matecconf/201824005006.

[24] T. Lewiński and G.I.N. Rozvany, “Exact analytical solutions for some popular benchmark problems in topology optimization III: L-shaped domains,” *Struct. Multidiscip. Optim.*, vol. 35, no. 2, pp. 165–174, Feb. 2008, doi: 10.1007/s00158-007-0157-8.

[25] N. Olhoff, J. Rasmussen, and M.P. Bendsøe, “On CADIntegrated Structural Topology and Design Optimization,” in *Evaluation of Global Bearing Capacities of Structures*, Vienna: Springer Vienna, 1993, pp. 255–280.

[26] A.G.M. Michell, “LVIII. The limits of economy of material in frame-structures,” *London, Edinburgh, Dublin Philos. Mag. J. Sci.*, vol. 8, no. 47, pp. 589–597, 1904, doi: 10.1080/14786440409463229.